Punching Shear Capacity of Double Layer FRP Grid Reinforced Slabs

by D.A. Jacobson, L.C. Bank, M.G. Oliva, and J.S. Russell

Synopsis: The punching shear capacity of concrete slabs reinforced with three-dimensional fiber-reinforced polymer (FRP) double-layer reinforcement cages composed of glass fiber-reinforced pultruded grating elements has been investigated using full-scale experimental tests and a number of different analytical models. Test specimens were full-scale prototype bridge deck slabs with varying end restraint and support conditions, differing dimensions, and two different FRP bar fiber lay-ups. The tests results were compared with the punching shear models in ACI 318, ACI 440, Eurocode 2, BS 8110, CEB-FIB MC90, JSCE, and a number of models proposed in the literature specifically for FRP reinforced slabs. Based on this investigation a new empirical model has been developed to predict the punching shear capacity of double layer grids having either restrained or simply supported edges and including an overlapping splice. The model is shown to give reasonably good predictions for both simply supported and restrained slabs.

Keywords: analysis; experiments; FRP; grids; modeling; pultrusion; punching shear; slabs

David Jacobson is a Design Engineer for the Structural Division of KPFF Consulting Engineers in Los Angeles, CA. He received his BS and MS degrees from the University of Wisconsin-Madison. His research interests include shear mechanisms in reinforced concrete and sustainable design.

ACI member **Lawrence Bank** is a Professor in the Department of Civil and Environmental Engineering at the University of Wisconsin-Madison. He is a member of ACI Committee 440. His research interests include analysis and design of FRP materials and structures in structural and construction engineering.

ACI member **Michael Oliva** is an Associate Professor in the Department of Civil and Environmental Engineering at the University of Wisconsin-Madison. His research interests include bridge design, prestressed concrete, and experimental dynamics.

Jeffrey Russell is a Professor in, and the Chair of, the Department of Civil and Environmental Engineering at the University of Wisconsin-Madison. His research interests include construction management, constructibility, and construction productivity

INTRODUCTION

The work presented in this paper forms part of a larger investigation to evaluate the use of an innovative FRP reinforcement system in a new concrete bridge deck measuring 130 by 45 ft (39.6 by 13.7 m) constructed in April 2004 on US Highway 151 over the De Nevue Creek in Fond du Lac, Wisconsin. As part of the design of the bridge deck experimental tests and modeling were performed to develop design guidelines for the FRP reinforcement system and to assist with the development of construction details. The FRP reinforcement system consists of very large double layer pultruded grids measuring 42.5 ft by 8 ft (13.0 by 2.4 m). Double layer pultruded grids have been studied in the past (Bank and Xi, 1993, 1995) and have been shown to have good potential as FRP reinforcements for decks from a cost and a performance perspective. This project was the first to apply the system to a new bridge deck. One of the key issues that needed to be investigated prior to the application of the system was developing an effective longitudinal splice between the FRP grid panels. Prior research (Bank and Xi, 1995) on small-scale slabs had proven the potential for a non-mechanically connected overlapping splice in the grid system. The critical load for a longitudinal splice (i.e., perpendicular to the girders) of this type is a concentrated wheel load that causes punching shear failure in the slab. This paper reports on the results of the study to investigate the punching shear capacity of slabs with longitudinal lap splices in the FRP double layer grids, and the behavior of the double layer grids, in general. The study included both experimental tests and analytical modeling of slabs with both simply supported and restrained (due to continuity over simulated girder supports) ends. In what follows the experimental work is described, the key results presented and comparisons with a number of existing code and proposed punching shear models for both steel reinforced slabs and FRP reinforced slabs are presented. A new empirical model that has been developed is then presented. The model shows good ability to predict punching

shear capacity of double layer FRP grid reinforced concrete slabs having either simply supported or restrained edges.

EXPERIMENTAL INVESTIGATION

Specimens

Five deck panel specimens were constructed. Each was 8" (200 mm) thick, with three of the test specimens (Specimens 1-3) measuring 6.5' x 7.5' (2.0 m x 2.3 m) and two (Specimens 7 and 8) measuring 6.5' x 14' (2.0 m x 4.3 m) [1]. Specimens 1-3 and 7 were cast outdoors at a concrete plant in northern Wisconsin. Specimen 8, was cast indoors at the University of Wisconsin over the upper portions of 54" (1372 mm) wide flange concrete I-girders to simulate actual bridge deck support conditions. A Wisconsin DOT Grade D, Size 1 (¾" (19 mm) max. aggregate size) concrete design mix, having a 28-day target compressive strength of 4,000 psi (27.6 MPa), was specified for all test specimens.

Deck reinforcement for the test specimens consisted of the modular double layer glass/vinylester pultruded FRP reinforcement cage (Fig. 1). Each bi-directional FRP grating layer of the reinforcement system was composed of pultruded 1.5" (38 mm) deep "I" bars spaced 4" (100 mm) on center as transverse reinforcement (perpendicular to deck supports) and pultruded locking cross rods, also spaced 4" (100 mm) on center and perpendicularly oriented to the I-bars, as longitudinal (temperature and shrinkage) reinforcement. The two layers were held together and spaced apart by FRP mechanical connector pieces. The mechanical connector pieces also served as "chairs" for the reinforcement cage system, spacing the bottom flanges of the lower grating layer 1" (25 mm) above the deck formwork. Concrete cover to the top flanges of the top grating layer was 1.5" (38 mm). The top and bottom grating layers were vertically spaced by a clear distance of 2.5" (64 mm). Due to the smooth finish on the FRP I-bars and locking cross-rods, very little bond is achieved between the concrete and FRP materials. However, the planar and perpendicular configurations of the FRP grid pieces mechanically anchor the reinforcement cage within the concrete every 4" at I-bar/cross rod intersections. In the bridge deck the transverse 1.5" (38 mm) I-bars are continuous over the bridge girders from one side of the bridge deck to the other. The cross rod pieces, or bridge longitudinal reinforcement, however, is spliced every 7' (2.1 m) longitudinally. Adjacent reinforcement cages are spliced together by means of a non-mechanically connected 12" (250 mm) overlap (Fig. 2), which provides continuity in the longitudinal direction.

The lap-splice region has been identified as the weakest part of the proposed bridge deck reinforcement system and therefore was included in all test specimens. The slabs were loaded at midpoint and the FRP reinforcement was designed to have the critical longitudinal splice at the edge of the critical perimeter of the loading footprint (Fig. 3).

---

[1] Specimens 4, 5 and 6 were flexural test specimens and are not discussed in this paper.

Test specimens 1-3 were placed on concrete support blocks and tested as simply supported slabs with a span of 6'6" (2.0 m). Specimens 7 and 8 were set-up to simulate a partial three-span configuration with deck continuity over two interior supports. Specimen 7 was centered on two concrete support blocks spaced 6'6" (2.0 m) center-to-center, which left overhangs of 3.75' (1.2 m) to the outside of each support. Specimen 8 was cast over the upper portions of two wide flange concrete precast girders (Wisconsin 54W, 54" (1372 mm) deep). This is the same girder section that was used in the bridge. The girder has 48" (1219 mm) wide top flanges. The girder supports were aligned and spaced to create 6'6" (2.0 m) from centerline-to-centerline, the same girder spacing as in the bridge. Due to the wide flanges of the girder supports, the actual clear span for the deck slab between the flange supports was 2'6" (0.8 m). Since the ends of test specimens 7 and 8 extended beyond the two interior supports, the overhanging ends were tied to the structural floor using a large steel frame and threaded rod in order to restrain them against upward displacement. This configuration was intended to better model actual bridge conditions and to study the effects of slab flexural end restraint on punching shear capacity.

Test Methods

Deflection measurements were taken with linear variable differential transformers (LVDTs) and strain potentiometers (Jacobson, 2004). Load cells measured all loads applied to the specimens. FRP and concrete material strains were recorded using electrical resistance strain gauges (see Jacobson, 2004 for details). Test loading was applied using a 200 kip (890 kN) capacity closed-loop servo hydraulic actuator, which was mounted vertically in a heavy steel frame that was bolted to a structural floor. A single patch load was applied to the center of each specimen using a 1.5" (38 mm) thick steel plate and a 2" (50 mm) thick neoprene rubber bearing pad with a length and width of 10" by 25" (250 by 635 mm).

Each specimen was subjected to manually-controlled monotonic loading until failure. Prior to the initiation of the ultimate capacity test, several monotonic service load cycles were run to document the cracking loads and behavior of the specimen through the service range (0-20.8 kips (0-92.5 kN)). In addition, one of the simply-supported specimens (Specimen 1) was subjected to fatigue cycling prior to the ultimate capacity portion of the test. The fatigue cycling was performed at 3 Hz as a sinusoidal wave load function peaking at 4.4 and 20.4 kips (19.6 and 90.7 kN). The 20.4 kip (90.7 kN) fatigue load was considered generally representative of the fatigue loads that the actual bridge deck might experience. A total of two million load cycles were conducted to simulate the fatigued condition of a bridge deck.

Test Results

The load deflection curves for the slabs are shown in Fig. 4. The ultimate capacities of the simply supported slabs (Specimens 1-3) correlated very well with each other; average capacity was 120.2 kips (535 kN) with a maximum difference of 1.2% from one another even though Specimen 1 had experienced an additional 2,000,000 cycles of fatigue load. The two flexurally-restrained specimens gave very different results from one another, due to differing support conditions. Specimen 7 failed at an ultimate

capacity of 162.2 kips (722 kN), while Specimen 8(with actual wide flange girder supports) carried an applied load of 201 kips (894 kN) when the test was ended. Unfortunately, the actuator's capacity was reached and complete failure was not achieved in Specimen 8, however radial punching shear cracks had developed on the top surface of the slab at the maximum load, which indicated an impending shear failure. All the results offered convincing evidence that the proposed FRP reinforcement cage system would perform well in the proposed bridge. In each case, the failure plane of the shear punch occurred through the lap-splice region of the FRP reinforcement cage. Fig. 5 shows a post-mortem section of one of the simply supported slabs where the failure "through" the lap splice region can be seen. Once a punch had begun, the splice would allow the specimen to "peel" apart at that region (due to no mechanical fasteners between spliced FRP reinforcement cages). This "peel" behavior was less pronounced in Specimen 7 due to the continuous and flexurally-restrained nature of the specimen ends. In addition, the punch area in Specimen 7 was cleaner and more defined, and more localized in comparison to the simply-supported tests (see Jacobson (2004) for more details and photographs of the failure surfaces).

Fatigue cycling did not appear to have an effect on the deck or the performance of the FRP reinforcement cage system, as residual deflections and stiffness loss due to fatigue cycling were minimal (Jacobson, 2004). This conclusion is substantiated by a close correlation in stiffness and nearly identical punching shear capacity test results from Specimens 1-3.

ANALYTICAL INVESTIGATION

In two-way reinforced concrete slabs the punching shear resistance is provided by the shear resistance of the concrete, V_c. This shear resistance acts over the area equal to the length of a "critical perimeter" multiplied by the effective depth of the section, d. The critical perimeter is identified by the letter u and a subscript that represents the distance that the critical perimeter is offset from the perimeter of the area of the concentrated load, as a multiple of the effective depth, d. For example, $u_{1.5}$ is the critical perimeter measured at a distance $1.5d$ from the edge of the loaded area. The following sections consider several models for V_c. The selected models were used to predict capacities for the slab test specimens, which were then compared to actual test ultimate capacities.

Punching Shear Models

A number of design standards provide punching shear design equations, typically for use with decks having steel reinforcement. Less is known about the punching shear behavior in concrete decks having FRP grid reinforcement systems. Similar to work performed by Banthia et al. (1995), Matthys and Taerwe (2000), El-Ghandour et al. (1997, 2003), and Ospina et al. (2003), an attempt is made to determine the best punching shear prediction model for the FRP grid-reinforced concrete bridge deck system used in this study.

ACI 318-02 – The punching shear capacity of a non-prestressed steel reinforced slab is given by the smallest of:

$$V_{ACI} = \left(2 + \frac{4}{\beta_c}\right)\sqrt{f_c'}u_{0.5}d$$

$$V_{ACI} = \left(\frac{\alpha_s d}{u_{0.5}} + 2\right)\sqrt{f_c'}u_{0.5}d \qquad (1)$$

$$V_{ACI} = 4\sqrt{f_c'}u_{0.5}d$$

where β_c is the ratio of the long side to short side of the rectangular concentrated load area, α_s is equal to 40 for interior slab loading, d and $u_{0.5}$ are the effective depth and critical section perimeter, respectively, and f_c' is the compressive strength of concrete in psi. The ACI equations are a function of the concrete strength and the surface area of an approximated shear failure plane and do not consider the deck reinforcement configuration, span, or slab end restraint. ACI's equations were empirically derived for concrete decks having mild steel reinforcement. For design, the nominal shear capacity is multiplied by the resistance factor, ϕ, however, for comparison with test results no resistance (or partial safety factors) were used in the calculations.

ACI 440 – The forthcoming (2005) revision of ACI 440.1R gives an equation for FRP reinforced slab punching shear capacity based on research by Ospina (2005) and Tureyen and Frosch (2003) given as,

$$V_{440} = 10k\sqrt{f_c'}u_{0.5}d \qquad (f_c' \text{ in psi})$$

$$\text{with}: k = \sqrt{2\rho\eta + (\rho\eta)^2} - \rho\eta \qquad (2)$$

$$\text{and} \quad \eta = \frac{E_f}{E_c} \quad \rho = \frac{A_f}{bd}$$

where, η is the FRP to concrete modular ratio and ρ is the FRP reinforcement ratio. The critical perimeter for the ACI 440 model is taken as $u_{0.5}$ similar to ACI 318.

Eurocode 2 (1992) – provides an empirical relationship that defines a bi-directional reinforcement ratio, ρ (where x and y denote the longitudinal and transverse directions of the reinforcement) and an averaged depth to the bottom layer reinforcement for the punching shear capacity of a steel reinforced slab as:

$$V_{EC2} = 0.25\frac{f_{ctk}}{\gamma_c}k_{EC}(1.2 + 40\rho)u_{1.5}d \qquad (3)$$

$$\text{with}: f_{ctk} = 0.7f_{ctm} \text{ and } f_{ctm} = 0.3\sqrt[3]{f_{ck}^2} \quad (f_{ck} \text{ in MPa})$$

$$k_{EC} = (1.6 - d) \geq 1 \quad (d \text{ in meters})$$

$$\rho = \sqrt{\rho_x\rho_y} \leq 0.15$$

The Eurocode 2 equation includes a partial safety factor, γ_c, which was set equal to 1.0 to get an unfactored prediction of the punching shear capacity. The mean value of tensile strength, f_{ctm} was used in place of the characteristic tensile strength, f_{ctk}, which corresponds to the 5%-fractile strength. The term f_{ck} represents the characteristic compressive strength of the concrete, which is equal to the mean compressive strength determined through cylinder testing, f_{cm} (basically the Eurocode's version of f'_c), minus 8 MPa for reliability of concrete strength. Eurocode's model does not consider slab end restraint.

BS 8110 – The British Standards Institution's BS 8110 gives the punching shear capacity for steel reinforced slabs as,

$$V_{BS} = \frac{0.79 k_1 k_2}{\gamma_m} \sqrt[3]{100\rho} \sqrt[4]{\frac{400}{d}} u_{1.5} d \quad (d \text{ in mm})$$

$$\text{with} : k_2 = \sqrt[3]{\frac{f_{ck}}{25}} \geq 1.0 \quad (f_{ck} \text{ in MPa})$$

$$0.0015 \leq \rho \leq 0.03 \tag{4}$$

$$\frac{400}{d} \geq 1.0$$

$$V_c \leq 0.8\sqrt{f_{ck}} u_{1.5} d \leq 5\, u_{1.5} d \quad (\text{MPa})$$

Like the Eurocode, BS 8110 includes a partial safety factor, γ_m which is set equal to 1.0. Variable k_1 is an enhancement factor for support compression and is conservatively taken as 1.0. As with the Eurocode 2 equations the mean compressive strength, f_{cm}, is used in place of the characteristic strength, f_{ck}.

CEB-FIP Model Code 1990 (MC90) – gives the punching resistance of a steel reinforced slab as the lesser of the following:

$$V_{MC90} = 0.12\xi\sqrt[3]{100\rho f_{ck}} u_{2.0} d \quad (d \text{ in meters; } f_{ck} \text{ in MPa})$$

$$\text{with} : \xi = 1 + \sqrt{\frac{0.2}{d}}$$

or $\tag{5}$

$$V_{MC90} = 0.3\left(1 - \frac{f_{ck}}{250} f_{cd} u_0 d\right)$$

MC90's equations incorporate the reinforcement ratio, ρ, but do not give consideration to span or slab end restraint variations. f_{cd} represents the concrete design strength, which in the case of MC90 is equal to the characteristic concrete strength, f_{ck}, divided by a partial safety factor, $\gamma_c = 1.5$. However, the characteristic concrete strength is substituted for the concrete design strength, f_{cd}, in Eq. (5) to obtain an unfactored punching shear capacity prediction. A partial safety factor is likely included in Eq. (5) as well, as part of the 0.12

constant (Matthys and Taerwe, 2000). Therefore, to get an unfactored prediction of punching shear capacity, the 0.12 constant was multiplied by partial safety factor of 1.5 to cancel out the integrated factor (0.18 used instead of 0.12).

JSCE – Japan's Society of Civil Engineering (JSCE) provides an empirically-based code equation for the punching shear capacity of FRP reinforced concrete decks. The JSCE relationship is tailored for use with FRP-reinforced concrete and incorporates the FRP to steel modular ratio directly. Like the other design equations discussed thus far, JSCE does not account for variations in span or slab end restraint. The JSCE equation is:

$$V_{JSCE} = \beta_d \beta_p \beta_r \frac{f_{pcd}}{\gamma_b} u_{0.5} d$$

$$\text{with}: \beta_d = \sqrt[4]{\frac{1}{d}} \leq 1.5 \qquad \beta_p = \sqrt[3]{100\rho \frac{E_f}{E_s}} \leq 1.5$$

$$\beta_r = 1 + \frac{1}{\left(1 + 0.25\frac{u_0}{d}\right)} \tag{6}$$

$$f_{pcd} = 0.2\sqrt{f_{cd}} \leq 1.2\,\text{MPa} \quad (f_{cd} \text{ in MPa})$$

$$\rho = \frac{A_f}{bd}$$

where γ_b is a partial safety factor generally equal to 1.3 (though equal to 1.5 if $f_{cd} > 50$ MPa) that was set equal to 1.0 to get an unfactored prediction of capacity. For this same reason, the design concrete compressive strength, f_{cd}, was replaced by the actual concrete compressive strength. The JSCE shear design equation uses the modular ratio of FRP to steel as a factor applied to the reinforcement ratio to account for the axial stiffness of the FRP.

In addition to the approaches recommended by the design codes presented above, there have been a number of empirically derived punching shear capacity equations developed by researchers through experimental programs. These proposed equations were developed specifically for FRP-reinforced concrete and are generally modifications of existing code equations.

Matthys and Taerwe (2000) – Their equation was based on information presented in

CEB Bulletin 168 (1985) and the punching shear equations in BS 8110.

$$V_{MT} = 1.36 \frac{\sqrt[3]{100\rho f_{cm}}}{\sqrt[4]{d}} u_{1.5} d \quad (d \text{ in mm}, f_{cm} \text{ in MPa}) \quad (7)$$

where f_{cm} is the mean concrete compressive strength.

El-Ghandour et al. (1999) – proposed an approach that incorporates an FRP to steel modular ratio to account for the lower axial stiffness of FRP, based on the ACI 440 equations for concrete shear strength in FRP-reinforced concrete:

$$V_{EPW} = 0.33\sqrt{f_c'} \sqrt[3]{\frac{E_f}{E_s}} u_{0.5} d \quad (f_c' \text{ in MPa}) \qquad (8)$$

Ospina et al. (2003) – refined the Matthys and Taerwe (2000) by adjusting a coefficient to provide an even better fit to the test data that they considered:

$$V_{OAC} = 2.77\sqrt[3]{\rho f_c'} \sqrt{\frac{E_f}{E_s}} u_{1.5} d \quad (f_c' \text{ in MPa})$$

$$\text{with} : \rho = \frac{A_f}{bd} \qquad (9)$$

where ρ is the FRP reinforcement ratio, f_c' is the concrete compressive strength, and E_f and E_s are the moduli of elasticity for FRP and steel, respectively.

In what follows the elastic modulus for concrete and the FRP reinforcement modulus are calculated using the following equations. The FRP modulus of elasticity considers the different FRP stiffnesses in the longitudinal and transverse directions and weights them according to cross-sectional area to get an averaged bi-directional modulus. The orientations "x" and "y" refer to the longitudinal or transverse reinforcements in the FRP panel (or I-bars and cross-rods):

$$E_c = 57000\sqrt{f_c'} \quad (f_c' \text{ in psi})$$

$$E_f = \frac{\rho_x E_{f(x)} + \rho_y E_{f(y)}}{\rho_x + \rho_y} \qquad (10)$$

Reinforcement Ratio Adjustments

Since most of the punching shear capacity equations presented above were developed for conventional steel-reinforced decks, it is reasonable to modify the equations to better represent the capacity of an FRP-reinforced slab. Previous research has shown that as the elastic stiffness of the flexural reinforcement decreases, the punching shear capacity of the slab also decreases Matthys and Taerwe, 2000, and Ospina et al., 2003).

Three different methods of determining the reinforcement ratio have been employed for each of the punching shear capacity equations presented earlier. The ACI 318 and the El-Ghandour equations are exceptions, as they do not incorporate the reinforcement ratio.

The punching shear equations proposed by ACI Committee 440, JSCE, Matthys and Taerwe, and Ospina et al. (2003) were developed specifically for use with the actual FRP reinforcement ratio and are not be used in conjunction with a modified reinforcement ratios presented in what follows.

Method 1 – The first method of determining the FRP reinforcement ratio, ρ_1, is the standard ratio of reinforcement area to deck concrete cross-sectional area defined by width, b, and effective section depth, d.

$$\rho_1 = \frac{A_f}{bd} \qquad (11)$$

Method 2 – The second method, ρ_2, is adopted from JSCE (1997) and also appears in design recommendations by Sonobe et al. (1997) factors the standard reinforcement ratio, ρ_1, by a modular ratio of FRP to steel to achieve an "equivalent" area of steel,

$$\rho_2 = \frac{A_f}{bd}\frac{E_f}{E_s} \qquad (12)$$

Method 3 – El-Ghandour et al. (2003) propose that the standard FRP reinforcement ratio, ρ_1, be multiplied by the FRP to steel ratios of strain and elastic moduli. They suggest a lower bound strain limit of 0.0045 for FRP reinforcements and 0.0025 for the yield strain of steel reinforcements.

$$\rho_3 = \phi_\varepsilon \frac{A_f}{bd}\frac{E_f}{E_s} \quad \text{with } \phi_\varepsilon = \frac{\varepsilon_f}{\varepsilon_{sy}} \qquad (13)$$

Since in the double layer grid considered in this study the reinforcement area is different in the longitudinal and transverse directions, an average of the two reinforcement ratios was used in the punching shear prediction calculations. An average ratio that is weighted by reinforcement stiffness was used for Method 1 and given as,

$$\rho_{ave} = \frac{\rho_x E_{f(x)} + \rho_y E_{f(y)}}{E_{f(x)} + E_{f(y)}} \qquad (14)$$

For Methods 2 and 3 the bi-directional reinforcement ratio recommended by the Eurocode 2 was used,

$$\rho_{ave} = \sqrt{\rho_x \rho_y} \qquad (15)$$

Properties for the Punching Shear Models

FRP material properties used in the punching shear equations were obtained from test data. Steel reinforcing bar properties were taken as f_y = 60 ksi (414 MPa) and E_s = 29,000 ksi (200 GPa); concrete strengths were obtained from cylinder tests. Tables 1 and 2 list the properties used in the punching shear capacity equations. I-bar cross-sectional

areas were calculated using the net area of the bar, that is, the gross area of the bar minus the area of the hole through the web for cross-rod insertion. Cross-rod areas were assumed equal to the holes through the I-bars (½" (12.6 mm) diameter). Only the bottom layer of grating reinforcement was considered in the calculation of punching shear capacity for the deck system. An extra set of slab properties from a series of tests conducted by Bank and Xi (1995) are included in the tables as this set of test data was included in the punching shear analysis to create a larger pool of results from which to draw conclusions. Bank and Xi performed tests on half-scale concrete slabs that utilized smaller, but very similar I-bar/cross-rod gratings as top and bottom layer reinforcements.

COMPARISON BETWEEN PREDICTED AND EXPERIMENTAL RESULTS

Tables 3 to 6 present ratios of test capacity to predicted capacity for each of the test specimens. Ratios of 1.0 perfectly predict the test capacity. Ratios higher than 1.0 show some level of conservativeness (i.e., safe), while ratios below 1.0 show that the model overestimates the shear capacity of the deck slab (i.e., unsafe). The tables are organized by the reinforcement ratio used in calculating the predicted capacities. For this reason, some models do not appear in all of the tables (such as ACI 318, which offers the same predicted capacity regardless of the reinforcement ratio). The results are grouped by test configuration type: simply-supported slabs (Specimens 1-3) and then the flexurally-restrained slabs (Specimens 7, 8 and Bank and Xi Specimens 1-6).

Looking only at the ratios calculated in Table 3 using the actual reinforcement ratio, ρ_1, none of the design code equations provide good predictions of capacity for the simply-supported specimens (Specimens 1-3). All but the ACI 440 approach overestimate the capacity of the simply supported slabs. This was expected given the reduced axial stiffness of the FRP reinforcements compared to steel. ACI 440 which was developed for FRP-reinforced concrete, provides a rather conservative prediction. Considering the flexurally-restrained slabs, the Eurocode and MC 90 code equations still tend to overestimate the capacity of the deck system. However, the other code equations provide conservative predictions, with the BS 8110 code equation showing the best fit to the data. The ACI 440 equation is shown to be overly conservative for the flexurally-restrained slabs, and at least for this body of test data, inferior to the original ACI 318 approach.

Of the approaches proposed by researchers, the equation by Ospina et al. (2003) provides the best predictions for the simply-supported slabs, but becomes quite conservative when applying the equation to the flexurally-restrained specimens. Conversely, the equation proposed by Matthys and Taerwe (2000) provides the best prediction for the flexurally-restrained slabs, but overestimates the capacity of the simply-supported slabs. The approach suggested by El-Ghandour et al. (1999) gives appropriately conservative predictions for the simply-supported test specimens, but becomes overly conservative when considering the flexurally-restrained specimens.

The ratios calculated using the modified reinforcement ratio, ρ_2, are shown in Table 4. The ACI 318, ACI 440, and El-Ghandour equations are not a function of the reinforcement ratio and do not yield a different prediction when ρ is varied therefore they

are not included. The JSCE equation appears here for the first time since it was developed for FRP-reinforced concrete using an actual reinforcement ratio multiplied by the modular ratio. The JSCE and MC90 code approaches both provide similar good capacity predictions for the simply-supported slabs. Like most of the approaches discussed thus far that provide good predictions for the simply-supported slabs, the JSCE equation becomes overly conservative when considering the flexurally-restrained slabs. The MC90 equation, however, provides reasonable though conservative predictions of capacity for the flexurally-restrained slabs. The reduction in reinforcement ratio caused the equation proposed by Matthys and Taerwe to become conservative with respect to Table 3.

The final table of test to predicted capacity ratios, Table 5, presents the capacity predictions using the modified reinforcement ratio, ρ_3. The reinforcement ratio is increased slightly over that used in Table 4, but it is still much less than the actual reinforcement ratio. The equation proposed by Matthys and Taerwe (2000) gives the best overall fit to this series of test capacities, with nearly perfect predictions for the simply-supported specimens and reasonably conservative predictions for the flexurally-restrained capacities.

NEW PUNCHING SHEAR MODEL FOR DOUBLE LAYER FRP GRATING REINFORCED SLABS WITH OVERLAP SPLICE

Each of the punching shear capacity models has been empirically derived for two-way slab action in which some level of edge restraint is present. However, no portion of any of the shear equations presented here directly incorporates the effect of varying levels of slab edge restraint, whether rotational or axial restraint. This is evident by the test to predicted capacity ratios; the tested spans of Specimens 1-3 and 7 are identical aside from the level of restraint present at the supported ends of the slab, yet the capacity ratios are not consistent. Additional research is necessary to fully consider and potentially model the effects of edge restraint on punching shear capacity. From this limited body of test results, no such model having an appropriate level of reliability can be proposed.

In general, ACI 318 offers a fair prediction of capacity for the flexurally-restrained slabs but overestimates the capacity for the simply-supported slabs. The punching shear equation proposed for the upcoming revised edition of the ACI 440 guidelines is shown to be overly conservative for all specimens, especially the flexurally-restrained slabs. The best models are shown to be the MC90 code equation used with the modular-modified reinforcement ratio ρ_2 and the approach proposed by Matthys and Taerwe (2000) used in conjunction with the reinforcement ratio modification ρ_3 proposed by El-Ghandour et al. (2003). These models provide capacity predictions that offered a nearly identical mean value and standard deviation for the entire body of test results. However, the modified reinforcement ratio suggested by El-Ghandour et al. (2003) assumes an ultimate strain of 0.0045 in the flexural reinforcement. Testing on Specimens 2 and 3 has shown that the tensile axial strains experienced at ultimate capacity in the FRP reinforcements of the bottom layer grating (<0.0031) were less than this seemingly arbitrarily set strain limit, and the calculated yield or rupture strains based on the

longitudinal strength and stiffness properties of the FRP are greater than 0.017 in/in. For this reason, the second modification of the FRP reinforcement ratio, ρ_3, will not be considered further, as the method appears to lack justification, at least for the FRP gratings considered in this research.

Based on a review of the results of the previously proposed models a new model is proposed by the University of Wisconsin (UW) for the punching shear resistance of glass/vinyletser mechanically-connected FRP double-layer pultruded grating-reinforced concrete slabs. The model is a modification of the empirical approach by Matthys and Taerwe (2000):

$$V_{UW} = 4.5 \frac{\sqrt[3]{\rho f_c'}}{\sqrt[4]{d}} u_{1.5} d \quad (d \text{ in mm}, f_c' \text{ in MPa})$$

$$\text{with} : \rho = \frac{A_f}{b\,d} \tag{16}$$

Variable ρ is the actual reinforcement ratio ρ_1, averaged and weighted for differing ratios in the main and distribution reinforcement directions according to Eq. (14). The critical perimeter, $u_{1.5}$, is representative of the top and bottom surface averaged failure perimeter seen in testing of Specimens 1-3, and 7.

The model nearly perfectly predicts the capacities of the simply-supported slabs, which means that for typical deck applications, where some level of edge restraint is involved, the calculated capacity will be conservative, but not overly conservative as shown in Table 6. In comparison to the empirical equations considered earlier, the proposed punching shear model provides the overall best fit to the entire body of test capacities considered.

CONCLUSIONS

A series of punching shear tests were performed on deck slab specimens reinforced with double layer glass/vinylester FRP pultruded grids having varying dimensions, support conditions, and end restraint conditions using a patch load that simulated the tire contact area of an HS-20 design truck double wheel. Punching shear was the mode of failure identified in all of the slab specimens. The punching shear capacity of the slab specimens was shown to be enhanced by introducing edge restraint to the specimens. In each case, the shear punch failure plane acted through the non-mechanically connected overlap splice between adjacent reinforcement cages. This confirmed the notion that the simple overlap splice would be the most structurally vulnerable aspect of the FRP reinforcement system, due to a lack of physical reinforcement continuity. It is important to note, though that this shear failure occurred through the splice region at loads many times greater than the HS-20 service load. No behavior was observed that would suggest that the overlap splice could jeopardize the structural adequacy and integrity of the FRP-reinforced deck system under truck traffic loading factored for impact per AASHTO Specifications.

An analysis of the punching shear strength of the FRP-reinforced slabs was performed using several empirically derived design models. The models, used to predict punching shear capacity, were evaluated based on the accuracy of the predictions relative to actual test capacities. Of the selected punching shear models, empirical approaches by the CEB-FIB Model Code 90 (1990) (using a reinforcement ratio modified to account for the axial stiffness of FRP) and by Matthys and Taerwe (2000) (also using a modified reinforcement ratio) yielded the best "fits" to the available slab data.

A new empirical equation based on the approach by Matthys and Taerwe (2000) has been proposed that provides an even better fit to the test data for double-layer glass/vinylester grating reinforced slabs. The new equation is recommended as it is derived especially for concrete slabs reinforced slabs reinforced with commercially available double layer FRP gratings with non-connected overlapping splices formed by offsetting the top and bottom grid panels. The applicability of the proposed equation to other heavy grid systems (such as NEFMAC) with similar overlapping splices or with different fiber types (such as carbon or aramid) or different grid intersections (such as integrally molded intersections) is not known at this time.

ACKNOWLEDGMENTS

REFERENCES

ACI 318, (2002). "Building Code Requirements for Structural Concrete and Commentary," *ACI 318-02,* American Concrete Institute, Farmington Hills, MI.

ACI 440, (2003). "Guide for the Design and Construction of Concrete Reinforced with FRP Bars," *ACI 440.1R-03*, American Concrete Institute, Farmington Hills, MI.

Bank, L.C. and Xi, Z. (1993). "Pultruded FRP Grating Reinforced Concrete Slabs," in *International Symposium on Fiber-Reinforced-Plastic Reinforcement for Concrete Structures*, Eds. A. Nanni and C.W. Dolan; American Concrete Institute (ACI SP-138), Detroit, MI, pp. 561-583.

Bank, L.C. and Xi, Z. (1995). "Punching Shear Behavior of Pultruded FRP Grating Reinforced Concrete Slabs," in *Second International RILEM Symposium on Non-Metallic (FRP) Reinforcement for Concrete Structures (FRPRCS-2)*, Ed. L Taerwe; E & FN Spon, London, pp. 360-367.

Banthia, N., Al-Asaly, M., and Ma, S. (1995). "Behavior of Concrete Slabs Reinforced with Fiber-Reinforced Plastic Grid," *Journal of Materials in Civil Engineering*, Vol. 7 , No. 4, pp. 252-257.

British Standards Institution (2002). "Part 1: Code of Practice for Design and Construction," *BS 8110-1:1997 Structural Use of Concrete*, London, UK.

Comité Euro-International du Béton (1993). "Design Code," *CEB-FIP Model Code 1990*, CEB, Lausanne, Switzerland.

El-Ghandour, A.W., Pilakoutas, K., Waldron, P. (1997). "Behavior of FRP Reinforced Concrete Flat Slabs," in *Third International RILEM Symposium on Non-Metallic (FRP) Reinforcement for Concrete Structures (FRPRCS-3)*, pp. 567-574.

El-Ghandour, A.W., Pilakoutas, K., Waldron, P. (2003). "Punching Shear Behavior of Fiber Reinforced Polymers Reinforced Concrete Flat Slabs: Experimental Study," *Journal of Composites for Construction*, Vol. 7, No. 3, pp. 258-265.

Jacobson, D.A., (2004), "Experimental and Analytical Study of Fiber Reinforced Polymer (FRP) Grid-Reinforced Concrete Bridge Decking," MS Thesis, University of Wisconsin, Madison.

Japan Society of Civil Engineers (1997). "Recommendation for Design and Construction of Concrete Structures Using Continuous Fiber Reinforcing Materials," *Concrete Engineering Series 23*, ed. by A. Machida, JSCE, Tokyo, Japan.

Matthys, S. and Taerwe, L. (2000). "Concrete Slabs Reinforced with FRP Grids. II: Punching Resistance," *Journal of Composites for Construction*, Vol. 4, No. 3, pp. 154-161.

Ospina, C.E. (2005). "Alternative Model for Concentric Punching in Capacity Evaluation of Reinforced Concrete Two-Way Slabs," *Concrete International*.

Ospina, C.E., Alexander, S.D.B., and Cheng, J.J.R. (2003). "Punching of Two-Way Slabs with Fiber-Reinforced Polymer Reinforcing Bars or Grids," *ACI Structural Journal*, Vol. 100, No. 5, pp. 589-598.

Sonobe, Y., et al. (1997). "Design Guidelines of FRP Reinforced Concrete Building Structures," *Journal of Composites for Construction*, Vol. 1, No. 3, pp. 90-115.

Tureyen, A.K. and Frosch, R.J. (2003). "Concrete Shear Strength: Another Perspective," *ACI Structural Journal*, Vol. 100, No. 5, pp. 609-615.

Table 1 – Slab Properties and Dimensions

	Specimen Number	Concrete Strength, f'_c psi (MPa)	Dimensions ft (m)	Slab depth in (mm)	Effective depth in (mm)
Tests	1	5507 (38)	6.5 x 7.5 (2.0 x 2.3)	8.0 (200)	6.33 (161)
	2	5343 (37)			
	3	5347 (37)			
	7	4973 (34)	6.5 x 14 (2.0 x 4.3)		
	8	7407 (51)			
Bank and Xi (1995)	1 – 6	4370 (30)	5 x 6 (1.5 x 1.8)	4.25 (108)	3.0 (76)

Table 2 – FRP Reinforcement Properties

	Specimen Number	I-bar		Cross-bar		I Bar /Cross bar spacing in (mm)	ρ_1 %	ρ_2 %	ρ_3 %
		Area in^2 (mm^2)	E_f ksi (GPa)	Area in^2 (mm^2)	E_f ksi (GPa)				
Tests	1	0.3221 (208)	4750 (33)	0.1963 (127)	6920 (48)	4/4 (100/100)	0.98	0.20	0.35
	2						0.98	0.20	0.35
	3						0.95	0.18	0.32
	7						0.98	0.20	0.35
	8						0.98	0.20	0.35
Bank and Xi (1995)	1	0.2221 (143)	4500 (31)	0.3068 (198)	5500 (38)	3/6 (75/150)	2.05	0.35	0.63
	2						2.05	0.35	0.63
	3						1.81	0.29	0.53
	4					3/6 (75/150)	2.05	0.35	0.63
	5	0.2421 (156)	4500 (31)	0.1963 (127)	5500 (38)		1.81	0.29	0.53
	6					6/6 (150/150)	1.49	0.25	0.45

Table 3 – Test to predicted punching shear capacity ratios for reinforcement ratio ρ_1

		Slab	Test (kips)	ACI 318 (eq1)	ACI 440 (eq2)	EC2 (eq3)	BS (eq4)	MC90 (eq5)	MT (eq7)	EPW (eq8)	OAC (eq9)
SS Slabs	Tests	1	120.8	0.75	1.82	0.46	0.80	0.60	0.71	1.18	1.03
		2	120.6	0.76	1.83	0.46	0.80	0.61	0.71	1.19	1.04
		3	119.3	0.75	1.92	0.47	0.80	0.61	0.71	1.22	1.09
		Ave		0.75	1.86	0.46	0.80	0.61	0.71	1.20	1.06
		SD		0.00	0.05	0.00	0.00	0.00	0.00	0.02	0.03
Restrained Slabs	Tests	7	162.2	1.06	2.51	0.67	1.11	0.84	0.98	1.66	1.43
		8	201.7	1.08	2.81	0.64	1.20	0.91	1.07	1.69	1.56
	Bank and Xi (1995)	1	41.8	1.58	3.07	0.84	1.03	0.74	0.92	2.88	1.72
		2	40.2	1.54	2.99	0.81	1.00	0.72	0.89	2.80	1.67
		3	44.7	1.71	3.55	0.91	1.16	0.83	1.03	3.14	1.96
		4	44.5	1.70	3.30	0.90	1.11	0.80	0.99	3.09	1.85
		5	45.2	1.73	3.58	0.91	1.17	0.84	1.04	3.17	1.98
		6	42.7	1.63	3.60	0.87	1.18	0.85	1.05	2.93	1.94
		Ave		1.50	3.18	0.82	1.12	0.82	1.00	2.67	1.77
		SD		0.26	0.37	0.10	0.07	0.06	0.06	0.59	0.19
All		Ave		1.30	2.82	0.72	1.03	0.76	0.92	2.27	1.57
		SD		0.40	0.67	0.18	0.15	0.11	0.14	0.82	0.35

Table 4 – Test to predicted punching shear capacity ratios for reinforcement ratio ρ_2

		Slab	Test (kips)	EC2 (eq3)	BS (eq4)	MC90 (eq5)	JSCE (eq6)	MT (eq7)
SS Slabs	Tests	1	120.8	0.58	1.36	1.03	1.04	1.21
		2	120.6	0.59	1.37	1.04	1.04	1.22
		3	119.3	0.58	1.40	1.07	1.07	1.22
		ave		0.58	1.38	1.05	1.05	1.25
		SD		0.01	0.02	0.01	0.02	0.02
Restrained Slabs	Tests	7	162.2	0.83	1.89	1.43	1.43	1.68
		8	201.7	0.79	2.06	1.56	1.74	1.83
	Bank and Xi (1995)	1	41.8	1.12	1.86	1.33	1.82	1.65
		2	40.2	1.09	1.81	1.29	1.77	1.60
		3	44.7	1.24	2.13	1.53	2.09	1.89
		4	44.5	1.21	2.00	1.43	1.96	1.77
		5	45.2	1.25	2.15	1.54	2.11	1.91
		6	42.7	1.20	2.15	1.54	2.11	1.91
		ave		1.09	2.01	1.46	1.88	1.78
		SD		0.17	0.13	0.10	0.22	0.12
All		ave		0.95	1.83	1.35	1.65	1.63
		SD		0.27	0.30	0.20	0.41	0.27

Table 5 – Test to predicted punching shear capacity ratios for reinforcement ratio ρ_3

		Slab	Test (kips)	EC2 (eq3)	BS (eq4)	MC90 (eq5)	JSCE (eq6)	MT (eq7)
SS Slabs	Tests	1	120.8	0.55	1.12	0.85	0.86	0.99
		2	120.6	0.56	0.56	1.13	0.86	1.00
		3	119.3	0.56	1.15	0.88	0.88	1.03
		ave		0.56	1.13	0.86	0.86	1.01
		SD		0.00	0.02	0.01	0.01	0.01
Restrained Slabs	Tests	7	162.2	0.79	1.55	1.18	1.18	1.38
		8	201.7	0.76	1.69	1.28	1.43	1.50
	Bank and Xi (1995)	1	41.8	1.04	1.53	1.09	1.49	1.36
		2	40.2	1.01	1.48	1.06	1.45	1.32
		3	44.7	1.15	1.75	1.26	1.72	1.56
		4	44.5	1.12	1.64	1.18	1.61	1.46
		5	45.2	1.17	1.77	1.27	1.73	1.57
		6	42.7	1.13	1.77	1.27	1.73	1.67
		ave		1.02	1.65	1.20	1.54	1.48
		SD		0.15	0.11	0.08	0.18	0.11
All		ave		0.89	1.51	1.11	1.36	1.35
		SD		0.24	0.25	0.17	0.34	0.23

Table 6 – Comparisons with Proposed Equation

		Slab	Test (kips)	Predicted (kips) (eq16)	$V_{test}/V_{predicted}$
SS Slabs	Tests	1	120.8	121.7	0.99
		2	120.6	120.5	1.00
		3	119.3	119.5	1.00
		ave			1.00
		SD			0.00
Restrained Slabs	Tests	7	162.2	117.6	1.38
		8	201.7	134.3	1.50
	Bank and Xi (1995)	1	41.8	32.2	1.29
		2	40.2	32.2	1.25
		3	44.7	30.9	1.45
		4	44.5	32.2	1.38
		5	45.2	30.9	1.46
		6	42.7	28.9	1.48
		ave			1.39
		SD			0.09
All		ave			1.29
		SD			0.19
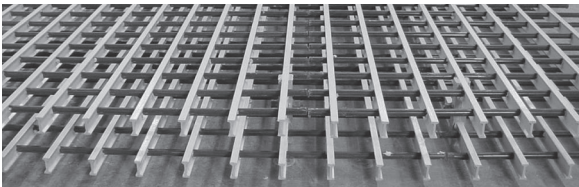
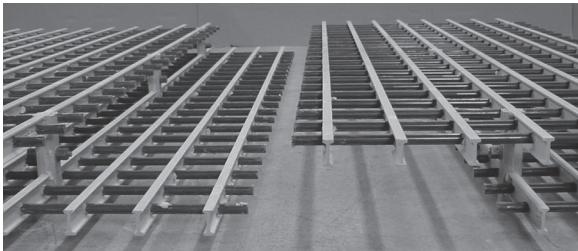Fig. 1 - Three dimensional double layer pultruded FRP grid

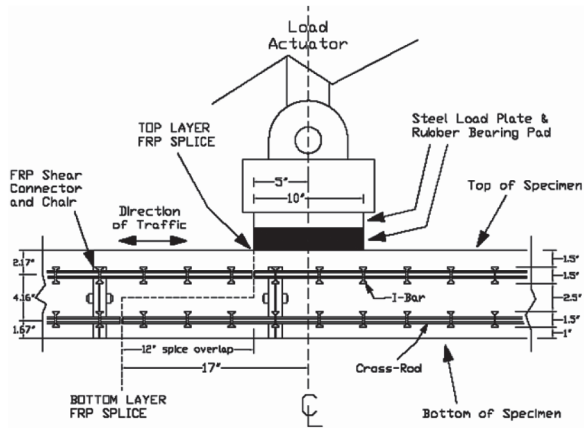Fig. 2 - Close-up view of longitudinal lap splice between two grids

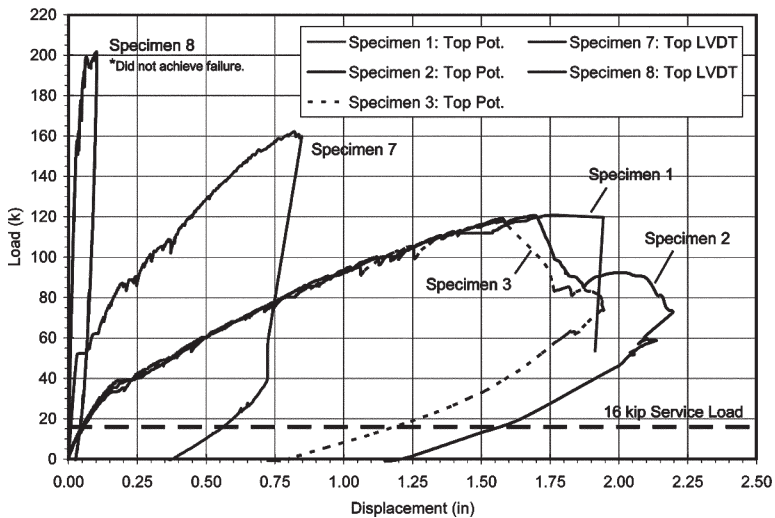Fig. 3 - Location of load patch relative to longitudinal splice

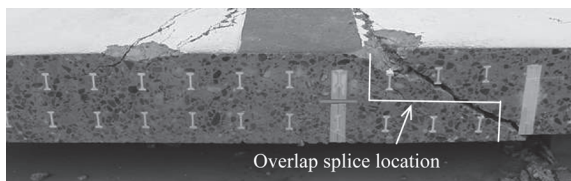Fig. 4 - Load-displacement curves for slab tests (1k = 1 kip = 4.445 kN, 1 in. = 25.4 mm)

Fig. 5 - Punching shear failure through splice region (post-mortem)